



# Synthesis, Single Crystal X-ray Structure Analysis and Computational Electronic Structure Investigations of 2-amino-7,7-dimethyl-4-(4-(methylthio)phenyl)-5-oxo-5,6,7,8-tetrahydro-4H-chromene-3-carbonitrile

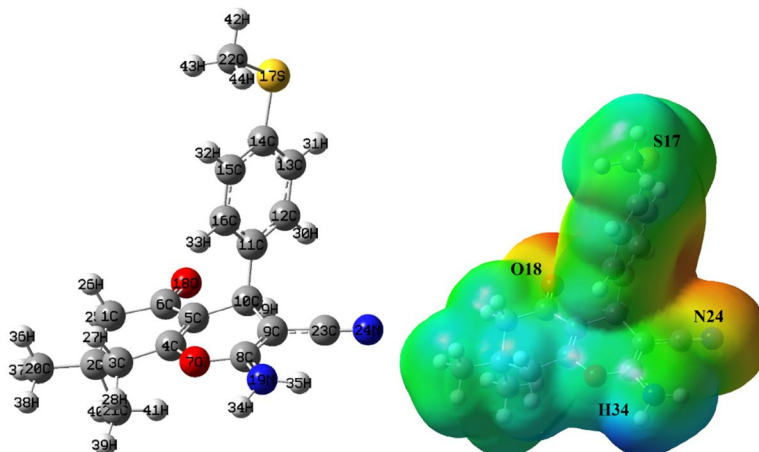
Ali Ramazani<sup>1,2</sup> · Hamideh Ahankar<sup>3</sup> · Katarzyna Ślepokura<sup>4</sup> · Tadeusz Lis<sup>4</sup> · Pegah Azimzadeh Asiabi<sup>1</sup> · Masoome Sheikhi<sup>5</sup> · Farideh Gouranlou<sup>6</sup> · Hooriye Yahyaei<sup>7</sup>

Received: 10 November 2017 / Accepted: 23 March 2019  
© Springer Science+Business Media, LLC, part of Springer Nature 2019

## Abstract

A clean, efficient and mild method is presented for one-pot three-component synthesis of 2-amino-7,7-dimethyl-4-(4-(methylthio)phenyl)-5-oxo-5,6,7,8-tetrahydro-4H-chromene-3-carbonitrile using nickel ferrite magnetic nanoparticles as a recyclable catalyst in green solvent at 40 °C. The structure of the target product was confirmed by FT-IR, <sup>1</sup>HNMR, <sup>13</sup>CNMR and single crystal X-ray structure analysis. In the present work, the quantum theoretical calculations of the molecular structure of this new compound have been predicted using Density Functional Theory in the solvent DMSO. The geometries of the title compound were optimized by B3LYP/6-31+G\* and B3LYP/6-311++G\*\* levels of theory. The electronic spectrum of the title compound in the solvent DMSO was carried out by TDB3LYP/6-311++G\*\* method. Frontier molecular orbitals, molecular electrostatic potential, electronic properties, natural charges and natural bond orbital analysis of the mentioned compound were investigated and discussed by theoretical calculations.

## Graphical Abstract



In the present work, the frontier molecular orbitals, molecular electrostatic potential, electronic properties, natural charges and Natural Bond Orbital (NBO) analysis of the mentioned compound were investigated and discussed by theoretical calculations.

**Electronic supplementary material** The online version of this article (<https://doi.org/10.1007/s10870-019-00778-5>) contains supplementary material, which is available to authorized users.

Extended author information available on the last page of the article

**Keywords** 4*H*-chromene · X-ray single crystal · Nickel ferrite · Magnetic nanoparticles · Green solvent

## Introduction

One of the most important of the class of polycyclic organic compounds is benzopyran, which has two isomers that are named 1-benzopyran (chromene) and 2-benzopyran (isochromene). Some structural frameworks containing the benzopyran nucleus with biological and pharmaceutical properties are chromane, 2*H*-chromene and specially 4*H*-chromene (Fig. 1) [1].

Different chromenes, such as vitamin E [2], cromakalim [3], conrauinone A [4], uvafzlelin [5] and erysenegalensein C [6], are marvelous class of compounds that are found in plenty of pharmaceuticals and active natural products. In addition, substituted chromenes have been known as interesting heterocyclic compounds with attractive pharmacological and biological properties as, e.g., anti-oxidant [2], anti-microbial and anti-fungal [7], anti-HIV [8], anti-tumor [9], anti-coagulant [10], anti-inflammatory [11], and diuretic [12] agents. Plus, some drugs with chromene moiety have been utilized for medical treatment of neurodegenerative diseases such as Alzheimer's, Down's syndrome and Parkinson's disease [13]. Moreover, compounds with chromene moiety are mostly employed in the arena of cosmetic and pigments industries [14].

Organic compounds containing sulfur are very numerous in the nature and often play an important role in various biochemical processes. The synthesis of a variety of sulfur-containing compounds have been investigated [15–22]. As part of our ongoing program to use of ferrite magnetic nanoparticles in multi-component reactions (MCRs) [23–26], in

this study we report an efficient and mild method for the synthesis of 2-amino-7,7-dimethyl-4-(4-(methylthio)phenyl)-5-oxo-5,6,7,8-tetrahydro-4*H*-chromene-3-carbonitrile in the presence of nickel ferrite magnetic nanoparticles (NiFe<sub>2</sub>O<sub>4</sub> MNPs) in a green solvent at 40 °C (Scheme 1).

In recent years, with the advances of quantum chemistry and development of fast computers, a new branch in chemistry has emerged, called computational chemistry. One of computational chemistry's main purpose is to create a computer program to calculate molecules properties including total energy, dipole moments, vibration frequencies and other known molecule properties. It can also be used in nuclear magnetic spectrometry.

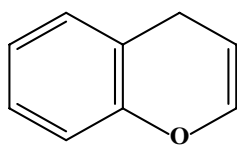
Theoretical quantum chemistry methods is an important area in determining the mechanisms of chemical reactions [27], especially catalysis [28], and structural determination of organic compounds [29]. Also, this method used for the prediction of spectroscopic data such as <sup>1</sup>H NMR and <sup>13</sup>C NMR chemical shifts [30], FT-IR, UV/Vis, and properties calculation of organic molecules [31].

In this research, we report the results of density functional theory (DFT) calculations to investigate absorption spectrum, UV/Vis, frontier molecular orbitals (FMO), molecular electrostatic potential (MEP), and natural bond orbital (NBO) of the new compound 2-amino-7,7-dimethyl-4-(4-(methylthio)phenyl)-5-oxo-5,6,7,8-tetrahydro-4*H*-chromene-3-carbonitrile. UV/Vis computations of new compound in the ground state were calculated by TD-DFT in a solvent DMSO.

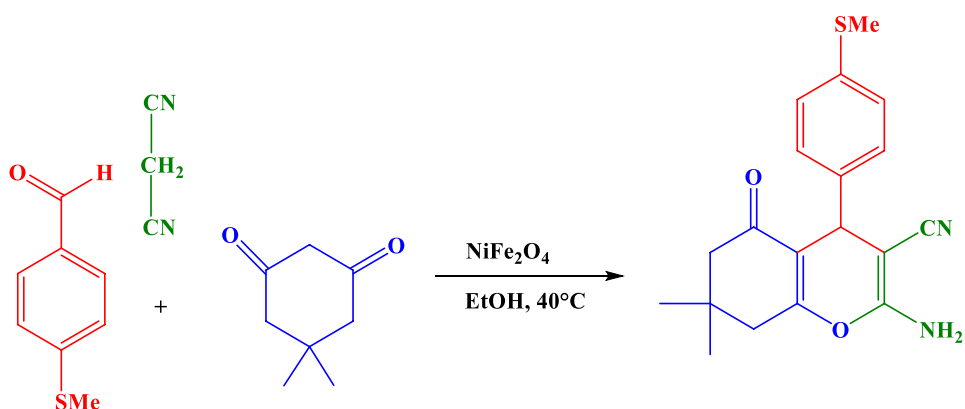
## Results and Discussion

The synthesis of 2-amino-7,7-dimethyl-4-(4-(methylthio)phenyl)-5-oxo-5,6,7,8-tetrahydro-4*H*-chromene-3-carbonitrile in the presence of prepared NiFe<sub>2</sub>O<sub>4</sub> MNPs [23] in a

**Fig. 1** Structure of 4*H*-chromene



**Scheme 1** Synthesis of 2-amino-7,7-dimethyl-4-(4-(methylthio)phenyl)-5-oxo-5,6,7,8-tetrahydro-4*H*-chromene-3-carbonitrile



green solvent at 40 °C was tested (Scheme 1). The proposed mechanism for the synthesis of 2-amino-7,7-dimethyl-4-(4-(methylthio)phenyl)-5-oxo-5,6,7,8-tetrahydro-4*H*-chromene-3-carbonitrile is shown in Scheme 2. First, Knoevenagel reaction in the presence of NiFe<sub>2</sub>O<sub>4</sub> MNPs, then, Michael addition and at the end, an intra-molecular cyclization of intermediate cause the target product.

The structure of the product was confirmed by <sup>1</sup>H NMR, <sup>13</sup>C NMR, and FT-IR spectroscopy. Melting points was also measured. Finally, single-crystal X-ray analysis of the product conclusively confirmed its structure (Fig. 2). The crystal of 2-amino-7,7-dimethyl-4-(4-(methylthio)phenyl)-5-oxo-5,6,7,8-tetrahydro-4*H*-chromene-3-carbonitrile was found to be isomorphous with the 4-(3-(trifluoro)phenyl) [32] and 4-(3,4-methylenedioxyphenyl) [33, 34] derivatives deposited at the CSD (Ver. 5.37, Feb. 2016) [35] with the refcodes MEWNAF and XOXZIT, XOXZIT01, XOXZIT02, respectively. Therefore, the molecular geometry of the title compound, as well as the packing of its crystal are very close to previously reported. The fused cyclohexene and pyran rings in 5,6,7,8-tetrahydro-4*H*-chromene moiety adopt *envelope* puckering (Cremer&Pople parameters [36]  $Q = 0.465(2)$  Å,  $\theta = 124.0(2)^\circ$ ,  $\Phi = 351.0(3)^\circ$ )

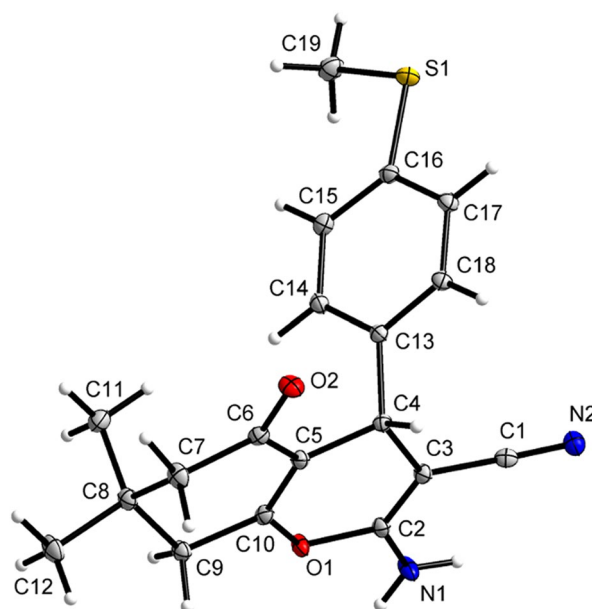
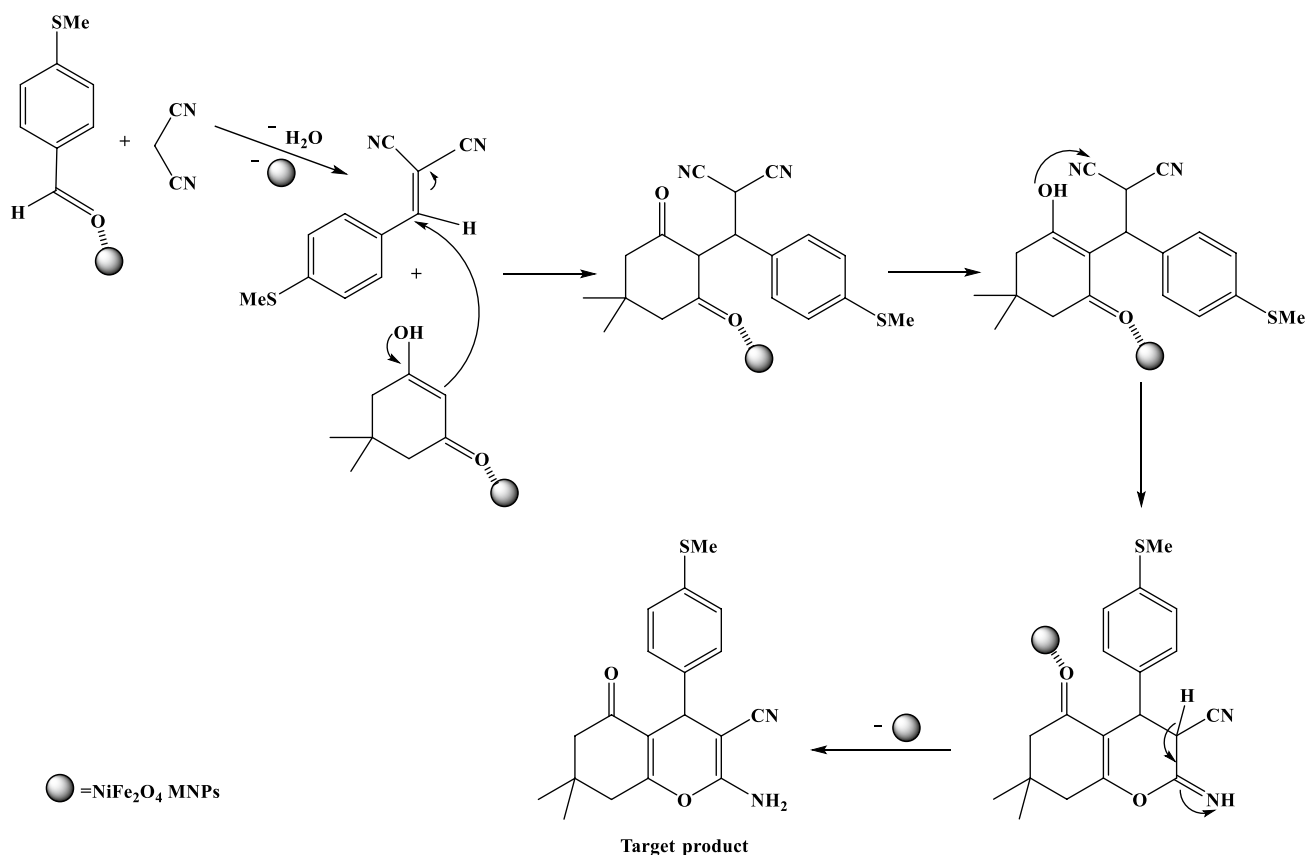


**Fig. 2** X-ray structure of 2-amino-7,7-dimethyl-4-(4-(methylthio)phenyl)-5-oxo-5,6,7,8-tetrahydro-4*H*-chromene-3-carbonitrile showing the atom-numbering scheme. The *S* enantiomer is shown. Displacement ellipsoids are drawn at the 50% probability level



**Scheme 2** The proposed mechanism for the synthesis of target product

and almost planar conformation (nearest puckering: *skew*;  $Q = 0.168(2)$  Å,  $\theta = 105.9(5)^\circ$ ,  $\Phi = 351.0(6)^\circ$ ). In the crystal lattice, molecular dimers are formed by the use of two centrosymmetric N–H $\cdots$ N interactions. Inter-dimeric N–H $\cdots$ O contacts provide further stabilization of the crystal and give rise to corrugated layers parallel to the (100) plane, as shown in Fig. 3. The methylthio groups are pointed towards the interlayer space.

## Computational Methods

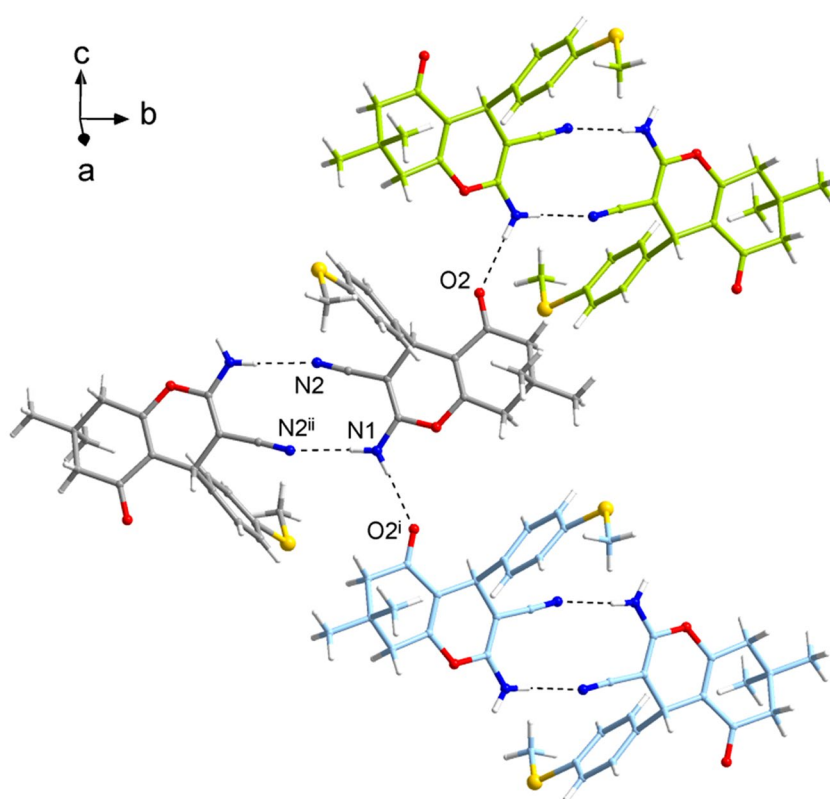
In this work, we have carried out quantum calculations and have optimized structure of the title compound using the DFT method with 6-31+G\* and 6-311++G\*\* basis sets by the Gaussian 09W program package [41] on a Pentium IV/4.28 GHz personal computer. We were also used from the Time Dependent Density Functional Theory (TD-DFT) for calculation of the electronic transitions of the title compound. The Polarized Continuum Model (PCM) [42] was used for calculations of solvent effect. Theoretical absorption spectrum of the structure in a solvent DMSO was calculated using the TD-DFT method. The electronic properties such as  $E_{\text{HOMO}}$ ,  $E_{\text{LUMO}}$ , energy gap between HOMO and LUMO, dipole moment ( $\mu_D$ ), point group and natural charge of the title structure were calculated [30]. The optimized molecular structure, HOMO and LUMO surfaces were visualized by

GaussView 05 program [43]. Also the electronic structure of the title compound were studied by NBO analysis [42] using B3LYP/6-311++G\*\* level of theory in order to understand hyperconjugative interactions and charge delocalization.

## Optimized Structure of the Title Compound

We carried out the DFT calculations for the title compound by B3LYP/6-31+G\* and B3LYP/6-311++G\*\* levels of theory in a solvent DMSO. The optimized molecular structure of the title compound is shown in Fig. 4. The quantum calculations were performed using the Gaussian 09 software package and GaussView 05 visualization programs on a Pentium IV/4.02 GHz personal computer. The integral equation formalism PCM (IEFPCM) coupled to UAKS radii is a method that was used to calculate the solvent (DMSO) effect. The IEFPCM, by Cancès, Mennucci and Tomasi is the most popular PCM version. It employs a molecule shaped cavity composed of spheres centered on the nuclei, while the reaction field is modeled by placing charges on the cavity surface. The selected experimental and calculated geometrical parameters such as bond lengths (Å) and bond angles ( $^\circ$ ) of the investigated structure have been obtained by B3LYP/6-31+G\* and B3LYP/6-311++G\*\* levels of theory and they are listed in Table 1.

**Fig. 3** Hydrogen bonds (dashed lines) in the crystal of 2-amino-7,7-dimethyl-4-(4-(methylthio)phenyl)-5-oxo-5,6,7,8-tetrahydro-4*H*-chromene-3-carbonitrile: centrosymmetric molecular dimers formed by the use of two N–H $\cdots$ N interactions, and the inter-dimeric N–H $\cdots$ O contacts. Geometry of H-bonds ( $D$ –H/Å, H $\cdots$ A/Å,  $D\cdots A$ /Å,  $D$ –H $\cdots A$ / $^\circ$ ) for N1–H1N $\cdots$ O2<sup>i</sup>: 0.81(2), 2.09(2), 2.9031(19), 178(2); for N1–H2N $\cdots$ N2<sup>ii</sup>: 0.86(3), 2.15(3), 3.008(2), 177(2). Symmetry codes: (i)  $x, -y + 1, z - 1/2$ ; (ii)  $-x, -y, -z$



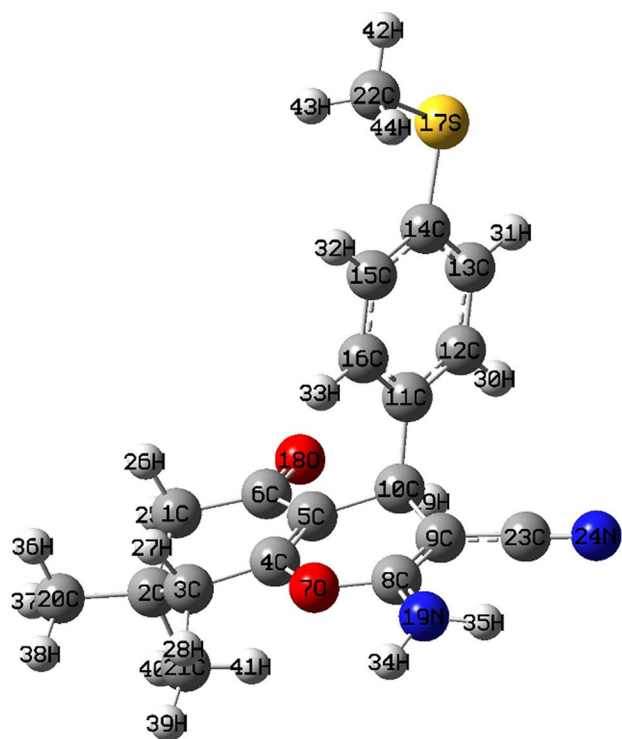


**Fig. 4** Optimized molecular structures of the title compound

From the Table 1, it has been observed that the calculated parameters show good approximation and can be used as a foundation to calculate the other parameters for the title compound. As can be seen from Table 1, the average differences of the theoretical parameters from the experimental for bond lengths of the title compound were found to be low. We found that most of the calculated bond lengths are slightly longer than X-ray values that it is due to the fact that experimental result corresponds to interacting molecules in the crystal lattice, whereas computational method deals with an isolated molecule in solvent phase [44]. The calculated C14–S17 bond length by 6-31+G\* and 6-311++G\*\* basis sets is 1.785 Å and 1.784 Å respectively, which are in good agreement with experimental value (1.763 Å). The calculated C8–N19 bond length in NO<sub>2</sub> group by 6-31+G\* and 6-311++G\*\* basis sets is 1.359 Å and 1.354 Å respectively and the experimental value is 1.332 Å, whereas the experimental C23–N24 bond length is 1.150 Å and the calculated values are 1.170 Å (by 6-31+G\*) and 1.161 Å (by 6-311++G\*\*). The C23–N24 bond length is shorter than the C8–N19 bond length that it is due to the C23–N24 bond is partly a triple bond, whereas the C8–N19 bond is doublet. The C13–C14–S17–C22 dihedral angle in the X-ray structure is 171.00° and the calculated bond angle by 6-31+G\* and 6-311++G\*\* basis sets is –179.67° and –179.76° respectively, therefore S–CH<sub>3</sub> group in the title compound with phenyl ring is in one plan.

**Table 1** Selected optimized geometrical parameters [Bond lengths (Å) and Bond angles (°)] of the title compound calculated by B3LYP/6-31+G\* and B3LYP/6-311++G\*\* methods

Parameter	Experimental	Calculated	
		B3LYP/6-31+G*	B3LYP/6-311++G**
<b>Bond lengths (Å)</b>			
C1–C2	1.538 (2)	1.545	1.543
C1–C6	1.506 (2)	1.519	1.516
C2–C3	1.532 (2)	1.547	1.545
C3–C4	1.490 (2)	1.497	1.495
C4–C5	1.338 (2)	1.351	1.346
C5–C6	1.469 (2)	1.473	1.472
C4–O7	1.376 (18)	1.374	1.373
O7–C8	1.371 (17)	1.366	1.364
C8–C9	1.364 (2)	1.367	1.363
C5–C10	1.501(2)	1.516	1.514
C9–C10	1.519 (2)	1.528	1.526
C2–C20	1.534 (2)	1.538	1.536
C2–C21	1.528 (2)	1.543	1.541
C6–O18	1.227 (18)	1.234	1.226
C8–N19	1.332 (2)	1.359	1.354
C9–C23	1.414 (2)	1.412	1.408
C23–N24	1.150 (2)	1.170	1.161
C10–C11	1.525 (2)	1.533	1.531
C11–C12	1.393 (2)	1.401	1.398
C11–C16	1.391(19)	1.399	1.396
C12–C13	1.386 (2)	1.394	1.390
C13–C14	1.401 (19)	1.405	1.401
C14–C15	1.393 (2)	1.402	1.399
C15–C16	1.395 (2)	1.397	1.394
C14–S17	1.763 (16)	1.785	1.784
S17–C22	1.7974 (17)	1.824	1.822
<b>Bond angles (°)</b>			
C1–C2–C3	108.28 (12)	108.19	108.21
C3–C4–C5	125.64 (13)	126.19	126.15
C3–C4–O7	111.11 (12)	111.45	111.47
C4–C5–C6	118.74 (13)	118.40	118.59
C4–O7–C8	118.62 (12)	119.68	119.66
O7–C8–C9	121.17 (13)	121.77	121.78
C5–C6–O18	119.68 (14)	120.93	120.96
O7–C8–N19	110.74 (13)	110.39	110.45
C9–C8–N19	128.09 (14)	127.80	127.74
C9–C10–C11	109.70 (12)	111.69	111.70
C8–C9–C23	119.22 (13)	118.92	118.99
C9–C23–N24	177.33 (15)	179.09	179.23
C11–C12–C13	121.56 (13)	121.25	121.23
C13–C14–C15	118.91 (13)	118.74	118.83
C13–C14–S17	116.20 (12)	116.88	116.87
C15–C14–S17	124.85 (11)	124.36	124.29
C14–S17–C22	103.65 (8)	104.06	104.01
C20–C2–C21	109.27 (12)	109.05	109.13

**Table 1** (continued)

Parameter	Experimental	Calculated	
		B3LYP/6-31+G*	B3LYP/6-311++G**
H34–N19–H35		114.83	115.86
Torsion angles (°)			
C4–C5–C6–O18	178.77 (13)	–173.17	–172.79
C10–C5–C6–O18	0.82 (19)	5.83	5.97
C4–O7–C8–C9	–6.58 (19)	7.56	7.81
C4–O7–C8–N19	173.52 (12)	–174.33	–173.69
C6–C5–C10–C11	–74.13 (16)	71.15	71.31
N19–C8–C9–C23	–0.8 (2)	6.48	6.30
C5–C10–C11–C16	–40.73 (19)	51.96	51.11
C9–C10–C11–C12	–92.78 (16)	107.17	106.28
C13–C14–S17–C22	171.00 (12)	–179.67	–179.76
C15–C14–S17–C22	–6.70 (15)	0.43	0.36

## Electronic Structure and Excited States of the Title Compound

We used the TD-DFT for predicting the absorption spectra of the title compound. The theoretical absorption spectrum of the optimized compound were calculated in a solvent DMSO by TDB3LYP/6-311++G\*\* method. 20 excited states considered for the calculation equations that were performed using the IEFPCM method coupled to UAKS radii. The exact amount of the maximum absorption wavelength ( $\lambda_{\max}$ ) to the title compound is obtained using the TD-DFT method.

20 excited states and wavelengths of electronic absorption spectrum of the title compound is reported in Table 2. As can be seen, the strong absorption at  $\lambda_{\max} = 226$  nm and the oscillator strength  $f = 0.18$  is due to charge transfer of electron into the excited state  $S_0 \rightarrow S_{16}$  with wave function including nine configurations [(H-1 $\rightarrow$ L), (H-1 $\rightarrow$ L), (H-1 $\rightarrow$ L), (H $\rightarrow$ L + 1), (H $\rightarrow$ L + 2), (H $\rightarrow$ L + 3), (H-1 $\rightarrow$ L + 4), (H $\rightarrow$ L + 6), (H $\rightarrow$ L + 8)]. The transition from HOMO to LUMO + 3 (H $\rightarrow$ L + 3) is main responsible for formation maximum wavelength at 226 nm (Table 2). Figure 5 shows shape molecular orbitals participants at  $\lambda_{\max} = 226$  nm. According to Fig. 2, the electron density of the HOMO is mainly focused on  $\text{C}=\text{C}$  in phenyl ring, the sulfur atom and methyl group (in  $\text{S}-\text{CH}_3$  group), whereas the LUMO is mainly focused on  $\text{-NH}_2$ ,  $\text{-CN}$ ,  $\text{-C}=\text{O}$  groups. Therefore the electronic transition from the HOMO to LUMO + 3 is mainly due to the contribution of pi ( $\pi$ ) bonds. The other important excited state is  $S_0 \rightarrow S_5$  at 266 nm ( $f = 0.17$ ) with two configurations for electronic excitations [(H-4 $\rightarrow$ L), (H-1 $\rightarrow$ L + 1), (H $\rightarrow$ L + 1), (H $\rightarrow$ L + 2)]. The other excited states of the title compound have very small intensity ( $f \approx 0$ ) that is nearly forbidden by orbital symmetry considerations

(Table 2). The calculated electronic absorption spectrum (UV/Vis) of the title compound in a solvent (DMSO) is observed in Fig. S4 in Supplementary Information.

## FMO Analysis of the Title Compound

The FMO analysis plays an significant role in the electronic and optical properties, as well as in UV/Vis spectrum and chemical reactions [42]. FMO analysis was done for the title compound by B3LYP/6-311++G\*\* level of theory. The FMO results of the title compound are summarized in Table 3.

The HOMO and LUMO orbitals act as electron donor and electron acceptor, respectively. As can be seen from Table 3, the energy values of the HOMO and LUMO of the title compound is  $-5.96$  eV and  $-1.92$  eV, respectively. Total electronic densities of states (DOSs) [45] of the title compound were computed (Fig. 6). The DOS analysis indicates that the energy gap between LUMO and HOMO of the title compound is about 4.04 eV.

A detail of quantum molecular descriptors of the title compound consist of ionization potential ( $I = -E_{\text{HOMO}}$ ), electron affinity ( $A = -E_{\text{LUMO}}$ ), global hardness ( $\eta = I - A/2$ ), electronegativity ( $\chi = I + A/2$ ), electronic chemical potential [ $\mu = -(I + A)/2$ ], electrophilicity ( $\omega = \mu^2/2\eta$ ) [30] and chemical softness ( $S = 1/\eta$ ) [42] are calculated and are reported in Table 3. The energy of HOMO is directly related to the ionization potential ( $I$ ), while the energy of LUMO is related to the electron affinity ( $A$ ). The global hardness ( $\eta$ ) corresponds to the energy gap between LUMO and HOMO. Electronegativity ( $\chi$ ) is a measure of the power of an atom or a group of atoms to attract electrons and the chemical softness ( $S$ ) describes the capacity of an atom or a group of atoms to receive electrons [42].

The dipole moment parameter is used for investigation of intermolecular interactions and study of asymmetric nature of compounds [30]. The high amounts of dipole moment lead to stronger intermolecular interaction [46]. As can be seen from Table 5, dipole moment value of the title compound is about 12.1621 Debye. The value of the dipole moment is related to the composition and dimensionality of the 3D compounds. The point group of the title compounds is C1, which refers to their high asymmetry. When the atoms in compound are irregularly arranged leads to the increasing dipole moment.

## MEP of the Title Compound

MEP maps show the electronic density in the molecules. The MEP maps are also used to identify sites of negative and positive electrostatic potentials for electrophilic attack

**Table 2** Electronic absorption spectrum of the title compound calculated by TDB3LYP/6-311++G\*\*

Excited State	Wave-length (nm)	Excitation energy (eV)	Configurations composition (corresponding transition orbitals)	Oscillator strength (f)
$S_1$	355	3.48	0.68(H→L)	0.05
$S_2$	323	3.83	0.68(H-1→L)	0.02
$S_3$	315	3.93	-0.13(H-4→L)+0.41(H-3→L)+0.49(H-2→L)+0.10(H-1→L)-0.13(H→L)	0.00
$S_4$	277	4.47	-0.10(H-2→L)+0.52(H→L+1)-0.40(H→L+2)	0.05
$S_5$	266	4.65	0.10(H-4→L)+0.10(H-1→L+1)-0.41(H→L+1)+0.52(H→L+2)	0.17
$S_6$	261	4.73	-0.21(H-4→L)+0.44(H-3→L)-0.43(H-2→L)+0.14(H-1→L+1)-0.17(H→L+1)	0.08
$S_7$	255	4.86	0.51(H-4→L)+0.12(H-3→L)+0.42(H-1→L+1)-0.15(H→L+2)	0.05
$S_8$	250	4.94	0.21(H-4→L)-0.29(H-1→L+1)+0.14(H-1→L+2)+0.36(H→L+3)+0.30(H→L+4)+0.26(H→L+5)	0.08
$S_9$	249	4.96	-0.29(H-4→L)+0.33(H-1→L+1)-0.27(H-1→L+2)-0.24(H→L+3)+0.32(H→L+4)+0.12(H→L+5)	0.02
$S_{10}$	247	5.01	-0.14(H-4→L)+0.27(H-1→L+1)-0.41(H-1→L+2)+0.43(H→L+3)	0.06
$S_{11}$	244	5.08	-0.22(H-1→L+2)+0.12(H-1→L+4)-0.10(H-1→L+8)+0.45(H→L+4)-0.30(H→L+5)+0.11(H→L+6)+0.25(H→L+7)-0.11(H→L+9)	0.00
$S_{12}$	241	5.13	-0.14(H-4→L)-0.12(H-3→L)+0.16(H-1→L+1)+0.33(H-1→L+2)-0.31(H-1→L+3)+0.27(H-1→L+8)+0.16(H→L+3)+0.20(H→L+4)+0.16(H→L+8)	0.06
$S_{13}$	234	5.29	0.26(H-1→L+3)-0.32(H-1→L+4)-0.15(H-1→L+6)+0.17(H-1→L+8)+0.12(H→L+5)+0.41(H→L+7)+0.15(H→L+8)+0.11(H→L+10)	0.00
$S_{14}$	233	5.30	0.11(H-4→L)-0.16(H-1→L+1)-0.29(H-1→L+2)+0.13(H-1→L+4)+0.41(H-1→L+8)-0.12(H→L+7)+0.30(H→L+8)	0.06
$S_{15}$	229	5.41	-0.25(H-1→L+3)+0.25(H-1→L+4)+0.12(H-1→L+6)-0.24(H→L+4)+0.18(H→L+5)+0.26(H→L+6)+0.33(H→L+7)+0.20(H→L+10)	0.00
$S_{16}$	226	5.48	0.23(H-1→L)-0.35(H-1→L)-0.11(H-1→L)+0.13(H→L+1)+0.28(H→L+2)+0.43(H→L+3)+0.22(H-1→L+4)+0.12(H→L+6)+0.10(H→L+8)	0.18
$S_{17}$	223	5.53	-0.15(H-5→L)-0.34(H-1→L+4)+0.54(H→L+6)-0.14(H→L+7)+0.10(H→L+9)	0.00
$S_{18}$	222	5.56	0.57(H-5→L)+0.10(H-3→L+1)+0.13(H-2→L+1)+0.12(H-2→L+2)-0.16(H-1→L+3)-0.15(H-1→L+4)	0.05
$S_{19}$	220	5.62	-0.19(H-5→L)+0.16(H-3→L+1)+0.59(H-2→L+1)+0.13(H-2→L+2)+0.11(H→L+8)	0.03
$S_{20}$	219	5.65	-0.19(H-1→L+8)-0.15(H→L+5)-0.12(H→L+6)+0.29(H→L+8)+0.46(H→L+9)+0.17(H→L+10)-0.14(H→L+13)	0.00

H HOMO, L LUMO

and nucleophilic reactions. The difference of the electrostatic potential at the surfaces is represented by different colors. The negative regions of MEP with red, orange and yellow color have the high electron density, while the positive regions with blue color have the low electron density. Also, the green color is shown neutral regions. The MEPs of the title compound was obtained by theoretical calculations (Fig. 7).

As shown in Fig. 7, the negative regions (red color) of the title compound are mainly focused on O18 atom, N24 atom and phenyl ring. Therefore, these regions are suitable for electrophilic attack. According to MEP map, the hydrogen atoms are the positive potential sites (blue color) and the most positive potential is mainly focused on H34 atom, therefore it is suitable for nucleophilic attack. The

regions with green color of the title compound indicate areas with zero potential (neutral sites).

### Natural Charge Analysis of the Title Compound

We calculated the charge distributions for equilibrium geometry of the investigated compound by the NBO (natural charge) charges [30] using B3LYP/6-31+G\* and B3LYP/6-311++G\*\* levels of theory. The calculated natural charges are listed in Table 4 (Atoms labeling is according to Fig. 7).

The total charge of the investigated compound is equal to zero. Also, Fig. 7 shows results of natural charges in graphical form. The results of natural charge (NBO)

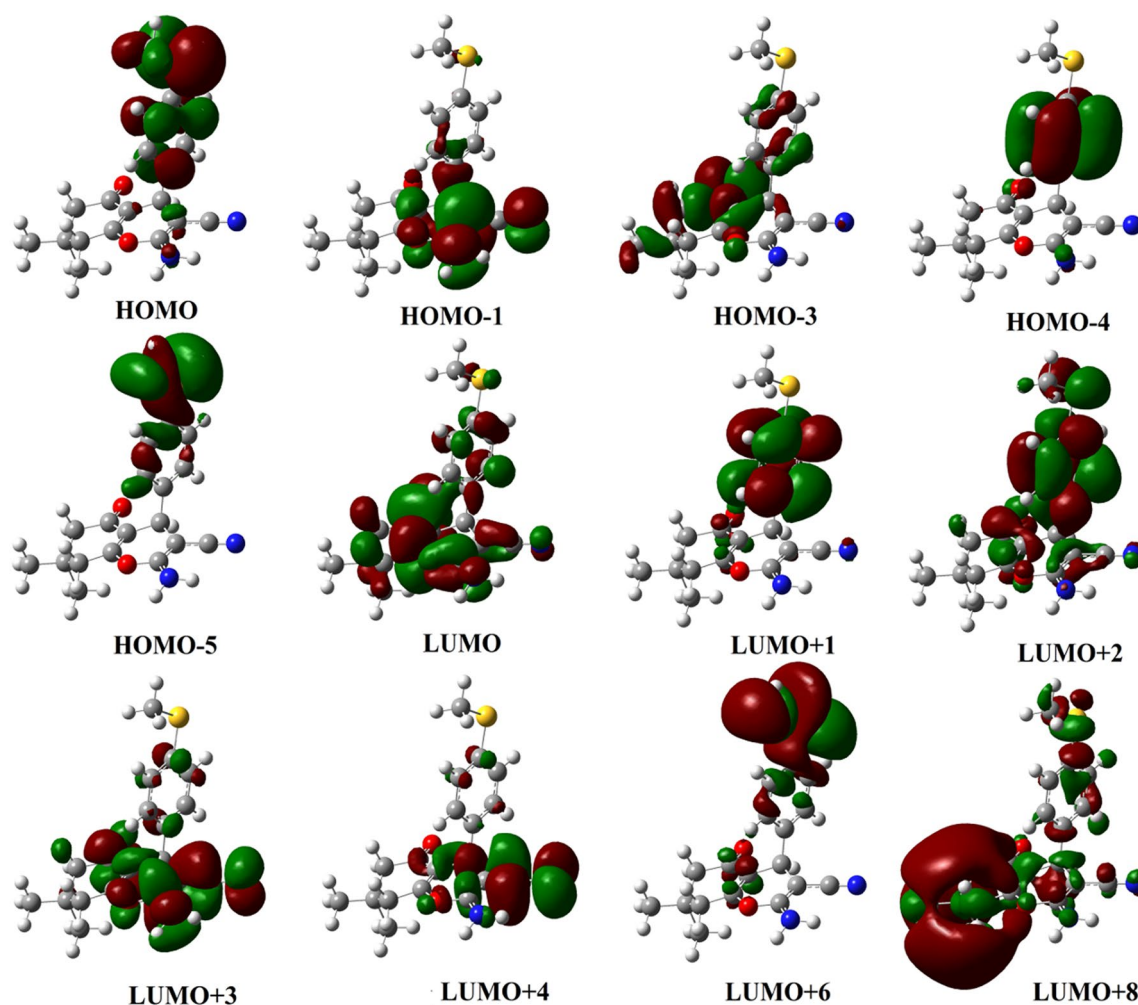


**Fig. 5** Form of the MO participant in formation of absorption spectrum of the title compound at  $\lambda_{\text{max}}=226$  nm calculated by B3LYP/6-311+G\*\* method

**Table 3** Electronic properties of the title compound calculated by B3LYP/6-311++G\*\* method

Property	B3LYP/6-311++G**
$E_{\text{HOMO}}$ (eV)	-5.96
$E_{\text{LUMO}}$ (eV)	-1.92
Energy gap (eV)	4.04
Ionisation potential, $I$ (eV)	5.96
Electron affinity, $A$ (eV)	1.92
Electronegativity, $\chi$ (eV)	3.94
Global hardness, $\eta$ (eV)	2.02
Chemical potential, $\mu$ (eV)	-3.94
Global electrophilicity, $\omega$ (eV)	3.84
Chemical softness, $S$ ( $\text{eV}^{-1}$ )	0.49
Dipole moment (Debye)	12.1621
Point group	C1

analysis show that carbon atoms have both positive and negative charges values. According to results, the positive carbons are observed for the carbons atoms attachment to the electron-withdrawing nitrogen and oxygen atoms. The C4, C6, C8, C10, C23 atoms have the positive charge and the other carbon atoms have negative charge. The oxygen and nitrogen atoms have negative charge. The highest positive charge of the compound is observed for C8 atom (0.583e by 6-31+G\* and 0.579e by 6-311++G\*\*) due to attachment to the electron-withdrawing O7 and N19 atoms. The C22 atom in the S-CH<sub>3</sub> group has the highest negative charge (-0.840e by 6-31+G\* and -0.706e by 6-311++G\*\*) rather than the other carbon atoms due to hyperconjugation effect. According to Natural charge's plot (Fig. S5 in Supplementary Information), all hydrogen atoms have the positive charge. The H34 and H35 atoms of

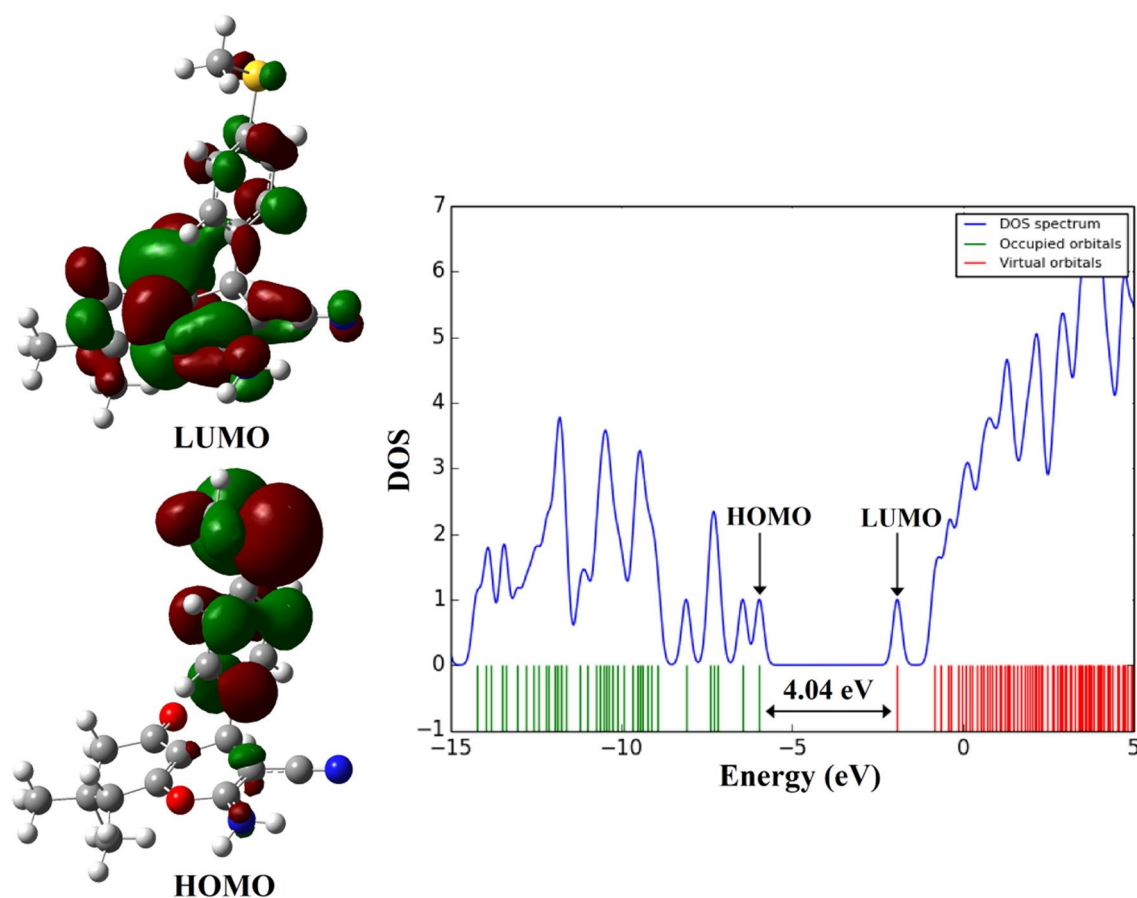


Fig. 6 Calculated DOS plots of the compound

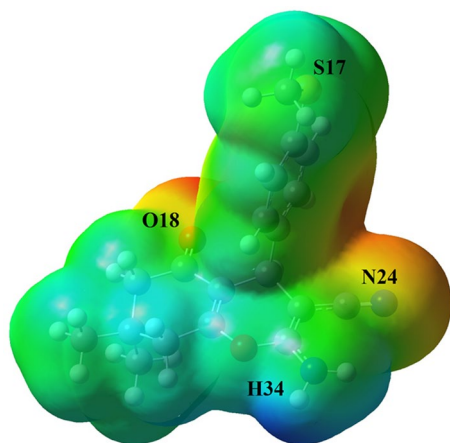


Fig. 7 MEP map of the title compound

the  $\text{NH}_2$  group have the highest positive charge (0.459e) rather than the other hydrogen atoms due to the

electron-withdrawing nature of the N19, therefore they are acidic hydrogens.

### NBO Analysis of the Title Compound

NBO analysis is important method for studying intra- and inter-molecular bonding and interaction between bonds in molecular systems [47]. Electron donor orbitals, acceptor orbitals and the interacting stabilization energy ( $E^{(2)}$ ) resulting from the second-order micro disturbance theory for the investigated compound are reported in Table 5.

The electron delocalization from filled NBOs (donor orbitals) to the empty NBOs (acceptor orbitals) describes a conjugative electron transfer process between them. For each donor ( $i$ ) and acceptor ( $j$ ), the stabilization energy  $E^{(2)}$  associated with the delocalization  $i \rightarrow j$  is estimated [42]:

$$E^{(2)} = \Delta E_{ij} = q_i \frac{F(i,j)^2}{\epsilon_j - \epsilon_i} \quad (1)$$

where  $q_i$  is the donor orbital occupancy,  $\epsilon_j$  and  $\epsilon_i$  are diagonal elements and  $F(i,j)$  is the off diagonal NBO Fock matrix

**Table 4** Natural Charges distribution (NBO charges, e) of the title compound using B3LYP/6-31+G\* and B3LYP/6-311++G\*\* methods

B3LYP/6-31+G*		B3LYP/6-311++G**		B3LYP/6-31+G*		B3LYP/6-311++G**	
Atoms	Charge	Atoms	Charge	Atoms	Charge	Atoms	Charge
C1	-0.533	C23	0.310	C1	-0.466	C23	0.307
C2	-0.098	N24	-0.423	C2	-0.065	N24	-0.432
C3	-0.501	H25	0.268	C3	-0.433	H25	0.229
C4	0.424	H26	0.276	C4	0.422	H26	0.237
C5	-0.195	H27	0.280	C5	-0.407	H27	0.240
C6	0.571	H28	0.275	C6	0.564	H28	0.236
O7	-0.499	H29	0.286	O7	-0.518	H29	0.228
C8	0.583	H30	0.252	C8	0.579	H30	0.215
C9	-0.325	H31	0.255	C9	-0.758	H31	0.218
C10	-0.268	H32	0.253	C10	0.576	H32	0.220
C11	-0.051	H33	0.249	C11	-0.143	H33	0.213
C12	-0.218	H34	0.449	C12	-0.187	H34	0.414
C13	-0.250	H35	0.450	C13	-0.223	H35	0.415
C14	-0.201	H36	0.242	C14	-0.178	H36	0.204
C15	-0.261	H37	0.245	C15	-0.238	H37	0.208
C16	-0.218	H38	0.244	C16	-0.193	H38	0.207
S17	0.249	H39	0.244	S17	0.239	H39	0.207
O18	-0.619	H40	0.245	O18	-0.619	H40	0.208
N19	-0.835	H41	0.241	N19	-0.764	H41	0.205
C20	-0.674	H42	0.276	C20	-0.569	H42	0.232
C21	-0.682	H43	0.259	C21	-0.579	H43	0.215
C22	-0.840	H44	0.259	C22	-0.706	H44	0.215

element. The resonance energy ( $E^{(2)}$ ) detected the quantity of participation of electrons in the resonance between atoms of molecule [42]. The larger  $E^{(2)}$  value, the more intensive is the interaction between electron donors and acceptor, i.e. the more donation tendency from electron donors to electron acceptors and the greater the extent of conjugation of the whole system. Delocalization of electron density between occupied Lewis-type (bond or lone pair) NBO orbitals and formally unoccupied (antibond or Rydberg) non Lewis NBO orbitals correspond to a stabilization donor–acceptor interaction. NBO analysis has been performed for the title compound by B3LYP/6-311++G\*\* method in order to elucidate the intramolecular, rehybridization, and delocalization of electron density within the title compound. We reported the highest strong intramolecular hyperconjugative interactions of the title compound such as  $\pi \rightarrow \pi^*$ ,  $\pi^* \rightarrow \pi^*$ ,  $\sigma \rightarrow \sigma^*$ ,  $n \rightarrow \sigma^*$  and  $n \rightarrow \pi^*$  transitions in Table 5. The  $\pi(\text{C14–C15})$  orbital in phenyl ring participates as donor and the anti-bonding  $\pi^*(\text{C11–C16})$ ,  $\pi^*(\text{C12–C13})$  and  $\pi^*(\text{C23–N24})$  orbitals act as acceptor with resonance energies ( $E^{(2)}$ ) 18.41 kcal/mol, 16.96 kcal/mol, and 109.33 kcal/mol, respectively. These values indicate  $\pi(\text{C14–C15}) \rightarrow \pi^*(\text{C23–N24})$  transition has the highest resonance energy (109.33 kcal/mol) compared with  $\pi(\text{C14–C15}) \rightarrow \pi^*(\text{C11–C16})$  and  $\pi(\text{C12–C13}) \rightarrow \pi^*(\text{C11–C16})$  transitions. The  $\pi(\text{C12–C13}) \rightarrow \pi^*(\text{C23–N24})$  transition has the highest resonance energy (156.29 kcal/mol) rather

than other  $\pi \rightarrow \pi^*$  transitions of the title compound. As can be seen from Table 6, the intramolecular hyperconjugative interactions of the  $\sigma \rightarrow \pi^*$  transitions have the higher resonance energy ( $E^{(2)}$ ) rather than the  $\pi \rightarrow \pi^*$  transitions. The  $\sigma(\text{C22–H42}) \rightarrow \pi^*(\text{C23–N24})$  transition has the highest resonance energy (992.48 kcal/mol) rather than other  $\sigma \rightarrow \pi^*$  transitions of the title compound. The  $\sigma(\text{C6–O18})$  orbital participates as donor and the anti-bonding  $\sigma^*(\text{C14–S17})$ ,  $\sigma^*(\text{C21–H41})$ ,  $\sigma^*(\text{C22–H44})$  orbitals act as acceptor with resonance energies ( $E^{(2)}$ ) of 92.42 kcal/mol, 57.50 kcal/mol and 562.58 kcal/mol, respectively. These values indicate  $\sigma(\text{C6–O18}) \rightarrow \sigma^*(\text{C22–H44})$  transition has the highest resonance energy (562.58 kcal/mol) rather than the  $\sigma(\text{C6–O18}) \rightarrow \sigma^*(\text{C14–S17})$  and  $\sigma(\text{C6–O18}) \rightarrow \sigma^*(\text{C21–H41})$  transitions. The highest resonance energy of the title compound is observed for  $\pi^*(\text{C14–C15}) \rightarrow \pi^*(\text{C23–N24})$  transition in with resonance energy ( $E^{(2)}$ ) 16475.83 kcal/mol that lead to most stability of the title compound. The most important transitions  $n \rightarrow \pi^*$  and  $n \rightarrow \sigma^*$  is observed for  $n2(\text{O7}) \rightarrow \pi^*(\text{C8–C9})$  and  $n1(\text{N19}) \rightarrow \pi^*(\text{C8–C9})$  with resonance energies ( $E^{(2)}$ ) 30.50 kcal/mol and 44.49 kcal/mol respectively. Also, the  $n2(\text{O18}) \rightarrow \sigma^*(\text{C1–C6})$  and  $n2(\text{O18}) \rightarrow \sigma^*(\text{C5–C6})$  transitions have the highest resonance energies about 17.61 kcal/mol and 17.89 kcal/mol respectively rather than other  $\sigma \rightarrow \sigma^*$  transitions of the title compound.

**Table 5** Significant donor–acceptor interactions and second order perturbation energies of the title compound calculated using the B3LYP/6-311+G\*\* level of energy

Donor (i)	Occupancy	Acceptor (j)	Occupancy	$E^{(2)a}$ kcal/mol	$E(j)-E(i)^b$ a.u.	$F(i, j)^c$ a.u.
$\pi(C4-C5)$	1.83628	$\pi^*(C6-O18)$	0.18223	22.70	0.31	0.075
$\pi(C8-C9)$	1.84351	$\pi^*(C23-N24)$	0.14349	104.29	0.09	0.086
$\pi(C11-C16)$	1.66707	$\pi^*(C12-C13)$	0.32038	21.24	0.29	0.070
$\pi(C12-C13)$	1.68333	$\pi^*(C11-C16)$	0.02584	20.48	0.28	0.069
		$\pi^*(C23-N24)$	0.14349	156.29	0.05	0.085
$\pi(C14-C15)$	1.66907	$\pi^*(C11-C16)$	0.02584	18.41	0.29	0.066
		$\pi^*(C12-C13)$	0.32038	16.96	0.30	0.064
		$\pi^*(C23-N24)$	0.14349	109.33	0.06	0.077
$\pi^*(C14-C15)$	0.41042	$\sigma^*(C14-S17)$	0.03284	852.54	0.52	1.260
		$\sigma^*(C21-H41)$	0.00625	412.24	0.77	1.102
		$\sigma^*(C22-H44)$	0.00469	3119.71	0.39	2.140
		$\pi^*(C23-N24)$	0.14349	16475.83	0.07	2.051
$\sigma(C1-H26)$	1.95369	$\sigma^*(C20-H36)$	0.00615	10.82	0.50	0.067
		$\sigma^*(C23-N24)$	0.14349	161.60	0.31	0.204
$\sigma(C5-C10)$	1.83317	$\sigma^*(C9-C10)$	0.12094	116.50	1.17	0.334
		$\sigma^*(C10-C11)$	0.05634	19.22	0.94	0.123
$\sigma(C6-O18)$	1.99420	$\sigma^*(C14-S17)$	0.03284	92.42	0.18	0.117
		$\sigma^*(C21-H41)$	0.00625	57.50	0.44	0.141
		$\sigma^*(C22-H44)$	0.01575	562.58	0.06	0.161
$\sigma(C11-C12)$	1.96893	$\sigma^*(C16-H33)$	0.01478	19.97	1.03	0.129
		$\sigma^*(C20-H36)$	0.00615	26.93	0.72	0.125
		$\sigma^*(C21-H41)$	0.00625	703.62	0.08	0.207
$\sigma(C14-C15)$	1.97774	$\sigma^*(C21-H41)$	0.00625	178.92	0.09	0.113
$\sigma(S17-C22)$	1.98926	$\sigma^*(C20-H36)$	0.00615	78.43	0.55	0.186
		$\sigma^*(C21-H39)$	0.00580	31.87	3.54	0.300
		$\sigma^*(C23-N24)$	0.14349	716.90	0.35	0.466
$\sigma(C22-H42)$	1.98862	$\sigma^*(C16-H33)$	0.01478	33.59	0.86	0.152
		$\sigma^*(C20-H36)$	0.00615	142.02	0.54	0.249
		$\sigma^*(C23-N24)$	0.14349	992.48	0.35	0.542
$n1(O7)$	1.96004	$\sigma^*(C4-C5)$	0.03145	5.32	1.20	0.071
		$\sigma^*(C8-C9)$	0.03012	5.10	1.15	0.068
$n2(O7)$	1.77969	$\pi^*(C4-C5)$	0.18247	27.80	0.39	0.094
		$\pi^*(C8-C9)$	0.34016	30.50	0.37	0.098
$n1(S17)$	1.98126	$\sigma^*(C14-C15)$	0.02719	3.79	1.19	0.060
		$\sigma^*(C20-H37)$	0.00562	5.31	0.99	0.065
$n2(S17)$	1.85599	$\sigma^*(C21-H39)$	0.00580	0.84	3.22	0.048
		$\pi^*(C23-N24)$	0.14349	3.42	0.03	0.10
$n1(O18)$	1.97796	$\sigma^*(C1-C6)$	0.05531	1.93	1.09	0.041
		$\sigma^*(C5-C6)$	0.06540	1.67	1.16	0.041
$n2(O18)$	1.89924	$\sigma^*(C1-C6)$	0.05531	17.61	0.67	0.098
		$\sigma^*(C5-C6)$	0.06540	17.89	0.73	0.103
$n1(N19)$	1.76465	$\sigma^*(C8-C9)$	0.03012	0.82	0.88	0.025
		$\pi^*(C8-C9)$	0.34016	44.49	0.31	0.108
$n1(N24)$	1.97087	$\sigma^*(C9-C23)$	0.02941	10.63	1.06	0.095

<sup>a</sup> $E^{(2)}$  Energy of hyperconjugative interactions<sup>b</sup>Energy difference between donor and acceptor i and j NBO orbitals<sup>c</sup> $F(i, j)$  Is the Fock matrix element between i and j NBO orbitals

**Table 6** Calculated NBO and the polarization coefficient for each hybrid in selected bonds of the title compound using the B3LYP/6-311++G\*\* level of theory

Occupancy (a.u.)	Bond (A–B) <sup>a</sup>	Energy (a.u.)	ED <sub>A</sub> (%)	ED <sub>B</sub> (%)	NBO	S(%) (A)	S(%) (B)	P(%) (A)	P(%) (B)
1.96598	σ(C1–C2)	–0.60386	49.88	50.12	0.7063 (sp <sup>2.39</sup> ) + 0.7080 (sp <sup>3.70</sup> )	29.52	24.54	70.44	75.41
1.97429	σ(C4–C5)	–0.77641	49.78	50.22	0.7055 (sp <sup>1.41</sup> ) + 0.7087 (sp <sup>1.72</sup> )	41.52	36.73	58.45	63.22
1.83628	π(C4–C5)	–0.30223	43.96	56.04	0.6630 (sp <sup>1.00</sup> ) + 0.7786 (sp <sup>99.99</sup> )	0.00	0.04	99.90	99.89
1.98775	σ(C4–O7)	–0.94006	30.46	69.54	0.5519 (sp <sup>3.38</sup> ) + 0.8339 (sp <sup>1.93</sup> )	22.75	34.09	77.00	65.85
1.99420	σ(C6–O18)	–1.09043	34.56	65.44	0.5879 (sp <sup>2.28</sup> ) + 0.8089 (sp <sup>1.35</sup> )	30.39	42.46	69.44	57.43
1.97373	π(C6–O18)	–0.38549	30.65	69.35	0.5536 (sp <sup>99.99</sup> ) + 0.8328 (sp <sup>99.99</sup> )	0.02	0.02	99.55	99.87
1.98587	σ(O7–C8)	–0.93825	68.37	31.63	0.8269 (sp <sup>2.18</sup> ) + 0.5624 (sp <sup>3.15</sup> )	31.41	24.01	68.52	75.74
1.98502	σ(C8–N19)	–0.87377	40.83	59.17	0.6390 (sp <sup>2.17</sup> ) + 0.7692 (sp <sup>1.66</sup> )	31.54	37.51	68.38	62.42
1.89568	σ(C10–C11)	–0.54672	46.17	53.83	0.6795 (sp <sup>2.79</sup> ) + 0.7337 (sp <sup>2.26</sup> )	26.33	30.62	73.52	69.36
1.96893	σ(C11–C12)	–0.73061	50.47	49.53	0.7104 (sp <sup>1.89</sup> ) + 0.7038 (sp <sup>1.77</sup> )	34.59	36.12	65.37	63.84
1.97984	σ(C14–S17)	–0.65693	53.65	46.35	0.7325 (sp <sup>2.92</sup> ) + 0.6808 (sp <sup>4.49</sup> )	25.50	18.11	74.36	81.28
1.98926	σ(S17–C22)	–0.56433	48.91	51.09	0.6994 (sp <sup>5.03</sup> ) + 0.7148 (sp <sup>3.48</sup> )	16.50	22.30	82.95	77.52
1.97472	σ(C2–C20)	–0.60350	52.07	47.93	0.7216 (sp <sup>2.85</sup> ) + 0.6923 (sp <sup>2.31</sup> )	25.97	30.22	73.99	69.75
1.99243	σ(C23–N24)	–1.06669	42.60	57.40	0.6527 (sp <sup>1.12</sup> ) + 0.7576 (sp <sup>1.12</sup> )	47.17	47.01	52.81	52.63
1.97462	σ(C23–N24)	–0.35259	41.82	58.18	0.6467 (sp <sup>1.00</sup> ) + 0.7627 (sp <sup>1.00</sup> )	0.00	0.00	99.91	99.70
1.95369	σ(C1–H26)	–0.51647	61.47	38.53	0.7840 (sp <sup>3.69</sup> ) + 0.6207 (s)	21.29	99.97	78.64	–
1.98276	σ(N19–H34)	–0.67544	70.86	29.14	0.8418 (sp <sup>2.62</sup> ) + 0.5398 (s)	27.58	99.93	72.37	–
1.98216	σ(N19–H35)	–0.68052	70.74	29.26	0.8411 (sp <sup>2.54</sup> ) + 0.5409 (s)	28.21	99.92	71.74	–
1.97792	σ(C12–H30)	–0.51726	60.84	39.16	0.7800 (sp <sup>2.54</sup> ) + 0.6258 (s)	28.21	99.95	71.74	–
1.98862	σ(C22–H42)	–0.55653	61.64	38.36	0.7851 (sp <sup>3.00</sup> ) + 0.6193 (s)	24.97	99.96	74.96	–
1.96004	n1(O7)	–0.57894	–	–	sp <sup>1.92</sup>	34.23	–	65.73	–
1.77969	n2(O7)	–0.36830	–	–	sp <sup>99.99</sup>	0.25	–	99.70	–
1.98126	n1(S17)	–0.63186	–	–	sp <sup>0.25</sup>	65.92	–	34.06	–
1.85599	n2(S17)	–0.24453	–	–	sp <sup>1.00</sup>	0.00	–	99.97	–
1.97796	n1(O18)	–0.70231	–	–	sp <sup>0.74</sup>	57.51	–	42.47	–
1.89924	n2(O18)	–0.27804	–	–	sp <sup>1.00</sup>	0.00	–	99.94	–
1.76465	n1(N19)	–0.30724	–	–	sp <sup>14.10</sup>	6.62	–	93.35	–
1.97087	n1(N24)	–0.52478	–	–	sp <sup>0.89</sup>	52.98	–	46.95	–

<sup>a</sup>A–B is the bond between atom A and atom B. (A: natural bond orbital and the polarization coefficient of atom; A–B: natural bond orbital and the polarization coefficient of atom B)

The results of NBO analysis such as the occupation numbers with their energies for the interacting NBOs [interaction between NBO A and NBO B (A–B)] and the polarization coefficient amounts of atoms in the title compound are presented using the B3LYP/6-311++G\*\* method is summarized in Table 6 (Atoms labeling is according to Fig. 7).

The size of polarization coefficients shows the importance of the two hybrids in the formation of the bond in molecules. The differences in electronegativity of the atoms involved in the bond formation are reflected in the larger differences in the polarization coefficients of the atoms (C–O, C–N, C–S, C–H bonds) [42]. As can be seen from Table 6, the calculated bonding orbital for the σ(C4–O7) bond is the σ = 0.5519(sp<sup>3.38</sup>) + 0.8339(sp<sup>1.93</sup>) with high occupancy 1.98775 a.u. and low energy –0.94006 a.u. The polarization coefficients of C4 = 0.5519 and O7 = 0.8339 shows

importance of O7 in forming σ(C4–O7) bond compared with C4 atom. As seen from Table 6, the calculated bonding orbital for the σ(C14–S17) bond is σ = 0.7325(sp<sup>2.92</sup>) + 0.6808(sp<sup>4.49</sup>) is formed from sp<sup>2.92</sup> and sp<sup>4.49</sup> hybrids on C14 and S17 atoms which is the mixture of s(25.50%) p(74.36%) for C14 and s(18.11%) p(81.28%) for S17. The natural hybrid orbital n2(O18) with high occupancy 1.89924 a.u. and high energy –0.27804 a.u. has p-character (99.94%). Therefore pure p-type lone pair orbital n2(O18) participates as electron donation to σ\*(C1–C6) and σ\*(C5–C6) in the n2(O18) → σ\*(C1–C6) and n2(O18) → σ\*(C5–C6) interactions with resonance energies (E<sup>(2)</sup>) 17.61 kcal/mol and 17.89 kcal/mol respectively (see Table 5). According to NBO analysis, the natural hybrid orbital n1(N19) occupy a high energy orbital (–0.30724 a.u.), high occupation number (1.76465 a.u) and high p-character (93.35%). Therefore

$n1(N19)$  participates as electron donation to  $\pi^*(C8-C9)$  in the  $n1(N19) \rightarrow \pi^*(C8-C9)$  interaction with high resonance energy ( $E^{(2)}$ ) 44.49 kcal/mol in the title compound (see Table 5).

## Experimental

### General

Starting materials were obtained from sigma-Aldrich, Merck, and Fluka were used without further purification. The method used to follow the reactions was TLC with UV light. Melting points were measured on an Electrothermal 9100 apparatus (LABEQUIP LTD., Markham, Ontario, Canada).  $^1H$  and  $^{13}C$  NMR (DMSO- $d_6$ ) spectra were recorded on a Bruker DRX-250 Avance spectrometer at 250.13 and 62.90 MHz, respectively. FT-IR spectrum was measured on a Jasco 6300 FT-IR spectrometer.

### Representative Procedure for Synthesis of 2-amino-7,7-dimethyl-4-(4-(methylthio) phenyl)-5-oxo-5,6,7,8-tetrahydro-4H-chromene-3-carbonitrile

A solution of 4-(methylthio) benzaldehyde (152 mg, 1 mmol), dimedone (140 mg, 1 mmol), malononitril (66 mg, 1 mmol) and ethanol (2 ml) was magnetically stirred at room temperature. To the mixture, prepared  $NiFe_2O_4$  MNPs [23] (5 mol %) was added and the content was heated at 40 °C for 60 min. The progress of the reaction was checked by TLC (n-hexane: EtOAc, 10:6). After completion, the resulting product was heated in ethanol. The catalyst was magnetically removed from the mixture and washed several times with acetone for reuse. The pure product was collected from the filtrate after cooling to room temperature with ice bath. The yield of isolated product was 90%. The pure product was obtained by recrystallization from hot ethanol. The Supplemental Information of sample, contain FT-IR (Fig. S1),  $^1H$  and  $^{13}C$  NMR spectra (Figs. S1 and S2), other Figs. and X-ray crystallography data.

### Spectral Data of Target Product

Colorless crystal (yield: 90%) M. P.: 239–242 °C. IR (KBr)  $\nu_{max}/cm^{-1}$ : 3355, 3257, 3188, 2963, 2192, 1683, 1652, 1369.  $^1H$  NMR (DMSO- $d_6$ , 250.13 MHz):  $\delta_H$  (ppm) 0.94 (s, 3H,  $CH_3$ ), 1.01 (s, 3H,  $CH_3$ ), 2.08 (d,  $J = 15.25$  Hz, 1H,  $CH_2$ ), 2.23 (d,  $J = 14.26$  Hz, 1H,  $CH_2$ ), 2.42 (s, 2H,  $CH_2$ ), 2.48 (s, 3H,  $SCH_3$ ), 4.14 (s, 1H, CH), 6.98 (s, 2H,  $NH_2$ ), 7.15 (d,  $J = 7.25$  Hz, 2H, Arom.), 7.09 (d,  $J = 7.00$  Hz, 2H, Arom.).  $^{13}C$  NMR (DMSO- $d_6$ , 62.90 MHz):  $\delta_C$  (ppm) 15.19, 27.27, 28.84, 32.22, 35.58, 50.44, 58.66, 113.09, 120.13, 126.43, 128.29, 136.55, 141.98, 144.19, 158.91, 162.84, 196.08.

### X-ray Crystallography

After recrystallization, pure solid of the title compound was dissolved in hot ethanol. X-ray crystals of desired product were obtained in excellent yield after evaporation of part of solvent at room temperature.

The crystallographic measurement was performed on an Xcalibur R  $\kappa$ -geometry automated four-circle diffractometer equipped with a CCD camera Ruby and graphite-monochromatized  $MoK\alpha$  radiation ( $\lambda = 0.71073$  Å). The data were collected at 80(2) K by using the *Oxford-Cryosystems* cooler. Data were corrected for Lorentz and polarization effects. Data collection, cell refinement, data reduction and analysis, and empirical (multi-scan) absorption correction were carried out with Xcalibur R software, *CrysAlisPro* [37]. As the title crystal is isomorphous with the crystals of 4-(3-(trifluoro)phenyl) [32] and 4-(3,4-methylenedioxyphenyl) [33, 34] derivatives (CSD refcodes MEWNAF and XOXZIT, XOXZIT01, XOXZIT02, respectively) [35], the refinement of its structure was started by using the coordinates of non-H atoms (except one O) taken from XOXZIT. The structure was refined by a full-matrix least-squares technique with *SHELXL2014* [38] and anisotropic thermal parameters for non-H atoms. All H atoms were found in difference Fourier maps and were refined isotropically. In the final refinement cycles, the C-bonded H atoms were repositioned in their calculated positions and refined using a riding model, with  $C-H = 0.95-1.00$  Å, and with  $U_{iso}(H) = 1.2U_{eq}(C)$  for CH and  $CH_2$  groups, or  $1.5U_{eq}(C)$  for  $CH_3$ . Amine H atoms were refined freely. Figures were made with the *DIAMOND* program [39]. Cremer–Pople puckering parameters were calculated using the *PLATON* program [40] Details of the conditions for the data collection and the structures refinements are given in Table 7 and the crystallographic information file (CIF) deposited with The Cambridge Crystallographic Data Centre (<http://www.ccdc.cam.ac.uk/>; deposition number CCDC-1564673) and provided as Supplementary Information.

### Conclusions

Briefly, an easy and convenient method was reported for the synthesis of 2-amino-7,7-dimethyl-4-(4-(methylthio) phenyl)-5-oxo-5,6,7,8-tetrahydro-4H-chromene-3-carbonitrile under mild conditions in the presence of  $NiFe_2O_4$  MNPs as a nanocatalyst. It should be noted, some significant advantages of this procedure are use of green solvent and catalyst, clean and environmentally benign conditions and clean. From the other important superiorities of this method are operational simplicity, easy work-up, non-chromatographic purification technique, short reaction time, and high yield.

**Table 7** Experimental details for the crystal

CCDC No.	1564673
Chemical formula	C <sub>19</sub> H <sub>20</sub> N <sub>2</sub> O <sub>2</sub> S
<i>M<sub>r</sub></i>	340.43
Crystal system, space group	Monoclinic, <i>C2/c</i>
Temperature (K)	80(2)
<i>a</i> , <i>b</i> , <i>c</i> (Å)	26.517(7), 9.197(3), 15.906(5)
$\beta$ (°)	118.57(4)
<i>V</i> (Å <sup>3</sup> )	3407(2)
<i>Z</i>	8
Radiation type	Mo <i>K</i> $\alpha$
$\mu$ (mm <sup>-1</sup> )	0.20
Crystal size (mm)	0.45 × 0.12 × 0.08
Absorption correction	Multi-scan
<i>T<sub>min</sub></i> , <i>T<sub>max</sub></i>	0.981, 1.000
No. of measured, independent and observed [ <i>I</i> > 2 $\sigma$ ( <i>I</i> )] reflections	9415, 4431, 3981
<i>R<sub>int</sub></i>	0.021
( <i>sin</i> $\theta$ / $\lambda$ ) <sub>max</sub> (Å <sup>-1</sup> )	0.720
<i>R</i> [ <i>F</i> <sup>2</sup> > 2 $\sigma$ ( <i>F</i> <sup>2</sup> )], <i>wR</i> ( <i>F</i> <sup>2</sup> ), <i>S</i>	0.044, 0.114, 1.11
No. of reflections	4431
No. of parameters	226
No. of restraints	0
$\Delta\rho_{max}$ , $\Delta\rho_{min}$ (e Å <sup>-3</sup> )	0.80, -0.35

Details in the crystallographic information file (CIF) provided as Supplementary Information

In the present study, the electronic structure of the new compound was modeled using the DFT calculations. From geometric parameter of the title compound, it is found that the experimental values are in good agreement with the calculated values. The maximum wavelength ( $\lambda_{max}$ ) in the electronic absorption spectrum of the title compound was observed at  $\lambda_{max} = 226$  nm. The C22 atom in the S-CH<sub>3</sub> group has the highest negative charge rather than the other carbon atoms and the H34 and H35 atoms of the NH<sub>2</sub> group have the highest positive charge rather than the other hydrogen. According to the results of NBO analysis, The highest resonance energy of the title compound is observed for  $\pi^*(C14-C15) \rightarrow \pi^*(C23-N24)$  transition in with resonance energy (*E*<sup>(2)</sup>) 16475.83 kcal/mol that lead to most stability of the title compound (Fig. S5).

**Acknowledgements** The Iranian authors are thankful to the “Iran National science Foundation: INSF” (Grant No. 95841255) for support of this work.

## References

- Ellis GP (1977) Chromenes, chromanones, and chromones. In: Ellis GP (ed) The chemistry of heterocyclic compounds chromenes vol 31. Wiley, Hoboken, p 1
- Reboul E, Richelle M, Perrot E, Desmoulins-Malezet C, Pirisi V, Borel P (2006) J Agric Food Chem 54(23):8749–8755
- Kudoh S, Okada H, Nakahira K, Nakamura H (1990) Anal Sci 6(1):53–56
- Victorine F, Augustin E (1998) J Nat Prod 61(3):380–383
- Hufford CD, Oguntimein BO, Van Engen D, Muthard D, Clardy J (1980) J Am Chem Soc 102(24):7365–7367
- Wandji J, Fomum ZT, Tillequin F, Libot F, Koch M (1995) J Nat Prod 58(1):105–108
- Raj T, Bhatia RK, Sharma M, Saxena A, Ishar M (2010) Eur J Med Chem 45(2):790–794
- Rueping M, Sugiono E, Merino E (2008) Chem Eur J 14(21):6329–6332
- Mohr SJ, Chirigos MA, Fuhrman FS, Pryor JW (1975) Cancer Res 35(12):3750–3754
- Manolov I, Maichle-Moessmer C, Danchev N (2006) Eur J Med Chem 41(7):882–890
- Moon D-O, Kim K-C, Jin C-Y, Han M-H, Park C, Lee K-J, Park Y-M, Choi YH, Kim G-Y (2007) Int Immunopharmacol 7(2):222–229
- Sharma U, Sharma U, Singh A, Agarwal V (2010) J Pharmacol Res 1(2):17–20
- Zhang YL, Chen BZ, Zheng KQ, Xu ML, Lei XH, Yaoxue XB (1982) Chem Abstr 96:135383e
- Hafez EAA, Elnagdi MH, Elagamey AGA, El-Taweel FMAA (1987) Heterocycles 26(4):903–907
- Ramazani A, Nasrabadi FZ, Ahankar H, Asiabi PA, Sadri F, Joo SW (2016) Phosphorus Sulfur Silicon Relat Elem 191(2):230–234
- Ramazani A, Nasrabadi FZ (2013) Phosphorus Sulfur Silicon Relat Elem 188(9):1214–1219
- Khoobi M, Ramazani A, Foroumadi A, Emami S, Jafarpour F, Mahyari A, Ślepokura K, Lis T, Shafiee A (2012) Helv Chim Acta 95(4):660–671
- Khoobi M, Foroumadi A, Emami S, Safavi M, Dehghan G, Alizadeh BH, Ramazani A, Ardestani SK, Shafiee A (2011) Chem Biol Drug Des 78(4):580–586
- Kazemizadeh AR, Ramazani A (2008) Arkivoc 15:159–165
- Ahankar H, Taheri S, Morsali A, Ramazani A, Zhu L-g (2006) J Coord Chem 59(18):2039–2045
- Amini I, Ramazani A, Ahankar H (2008) Phosphorus Sulfur Silicon 183(8):1994–1999
- Rahnema M, Bigdeli MR, Kazemizadeh AR, Ramazani A (2007) Phosphorus Sulfur Silicon Relat Elem 182(8):1683–1688
- Ahankar H, Ramazani A, Joo SW (2016) Res Chem Intermed 42(3):2487–2500
- Taghavi Fardood S, Ramazani A, Moradi S (2017) J Sol-Gel Sci Technol 82:432–439
- Taghavi Fardood S, Ramazani A, Golfar Z, Joo SW (2017) Appl Organomet Chem 31:e3823. <https://doi.org/10.1002/aoc.3823>
- Khoobi M, Ma’mani L, Rezazadeh F, Zareie Z, Foroumadi A, Ramazani A, Shafiee A (2012) J Mol Catal A 359:74–80
- Parr RG, Yang W (1984) J Am Chem Soc 106(14):4049–4050
- Shahab S, Filippovich L, Kumar R, Darroudi M, Borzemandani MY, Gomar M, Hajikolaee FH (2015) J Mol Struct 1101:109–115
- Shahab S, Filippovich L, Sheikhi M, Yahyaei H, Aharodnikova M, Kumar R, Khaleghian M (2017) Am J Mater Synth Process 5(2):17–23
- Sheikhi M, Sheikh D, Ramazani A (2014) S Afr J Chem 67:0–0
- Shahab S, Filippovich L, Sheikhi M, Kumar R, Dikuser E, Yahyaei H, Muravsky A (2017) J Mol Struct 1141:703–709

32. Kant R, Gupta VK, Kapoor K, Patil D, Chandam D, Deshmukh MB (2013) *Acta Cryst E* 69(3):o417–o418
33. Wang X-S, Shi D-Q, Tu S-J, Yao C-S (2003) *Synth Commun* 33(1):119–126
34. Brahmachari G, Banerjee B (2013) *ACS Sustain Chem Eng* 2(3):411–422
35. Groom CR, Allen FH (2014) *Angew Chem Int Edit* 53(3):662–671
36. Cremer zt, Pople J (1975) *J Am Chem Soc* 97(6):1354–1358
37. CrysAliPRO in Xcalibur R software., Agilent Technologies, Yarnton, Oxfordshire, England (2012)
38. Sheldrick GM (2015) *Acta Crystallogr Sect C* 71(1):3–8
39. Brandenburg K (2014) DIAMOND Version 32 k Crystal Impact GbR. Bonn, Germany
40. Spek AL (2009) *Acta Crystallogr Sect D* 65(2):148–155
41. Frisch M, Trucks G, Schlegel H, Scuseria G, Robb M, Cheeseman J, Scalmani G, Barone V, Mennucci B, Petersson G (2009)
42. Shahab S, Sheikhi M, Filippovich L, Anatol'evich DE, Yahyaei H (2017) *J Mol Struct* 1137:335–348
43. Frisch A, Nielsen AB, Holder AJ, GVUM Gaussian Inc., (2008)
44. Saeed S, Rashid N, Jones PG, Ali M, Hussain R (2010) *Eur J Med Chem* 45(4):1323–1331
45. Sheikhi M, Shahab S, Filippovich L, Khaleghian M, Dikumar E, Mashayekhi M (2017) *J Mol Struct* 1146:881–888
46. Sheikhi M, Sheikhi D (2014) *Rev Roum Chim* 59(9):761–767
47. Weinhold F, Landis CR (2001) *ChemEduc Res Prac* 2(2):91–104

**Publisher's Note** Springer Nature remains neutral with regard to jurisdictional claims in published maps and institutional affiliations.

## Affiliations

Ali Ramazani<sup>1,2</sup>  · Hamideh Ahankar<sup>3</sup> · Katarzyna Ślepokura<sup>4</sup> · Tadeusz Lis<sup>4</sup> · Pegah Azimzadeh Asiabi<sup>1</sup> · Masoome Sheikhi<sup>5</sup> · Farideh Gouranlou<sup>6</sup> · Hooriye Yahyaei<sup>7</sup>

✉ Ali Ramazani  
aliramazani@gmail.com; aliramazani@znu.ac.ir

✉ Hamideh Ahankar  
hahankar@gmail.com

<sup>1</sup> Department of Chemistry, University of Zanjan, P O Box 45195-313, Zanjan, Iran

<sup>2</sup> Research Institute of Modern Biological Techniques, University of Zanjan, P O Box 45195-313, Zanjan, Iran

<sup>3</sup> Department of Chemistry, Abhar Branch, Islamic Azad University, P O Box 22, Abhar, Iran

<sup>4</sup> Faculty of Chemistry, University of Wrocław, 14 Joliot-Curie St, 50-383 Wrocław, Poland

<sup>5</sup> Young Researchers and Elite Club, Gorgan Branch, Islamic Azad University, Gorgan, Iran

<sup>6</sup> Department of Bioscience and Biotechnology, Malek Ashtar University of Technology, Tehran, Iran

<sup>7</sup> Department of Chemistry, Zanjan Branch, Islamic Azad University, Zanjan, Iran